ER stress and distinct outputs of the IRE1α RNase control proliferation and senescence in response to oncogenic Ras

Nicholas Blazanin[a,1], Jeongin Son[a], Alayna B. Craig-Lucas[a], Christian L. John[a], Kyle J. Breech[a], Michael A. Podolsky[a,2], and Adam B. Glick[a,3]

[a]Department of Veterinary and Biomedical Sciences, The Center for Molecular Toxicology and Carcinogenesis, The Pennsylvania State University, University Park, PA 16802

Edited by Kevan M. Shokat, University of California, San Francisco, CA, and approved August 1, 2017 (received for review February 13, 2017)

Oncogenic Ras causes proliferation followed by premature senescence in primary cells, an initial barrier to tumor development. The role of endoplasmic reticulum (ER) stress and the unfolded protein response (UPR) in regulating these two cellular outcomes is poorly understood. During ER stress, the inositol requiring enzyme 1α (IRE1α) endoribonuclease (RNase), a key mediator of the UPR, cleaves *Xbp1* mRNA to generate a potent transcription factor adaptive toward ER stress. However, IRE1α also promotes cleavage and degradation of ER-localized mRNAs essential for cell death. Here, we show that oncogenic HRas induces ER stress and activation of IRE1α. Reduction of ER stress or *Xbp1* splicing using pharmacological, genetic, and RNAi approaches demonstrates that this adaptive response is critical for HRas-induced proliferation. Paradoxically, reduced ER stress or *Xbp1* splicing promotes growth arrest and premature senescence through hyperactivation of the IRE1α RNase. Microarray analysis of IRE1α- and XBP1-depleted cells, validation using RNA cleavage assays, and 5′ RACE identified the prooncogenic basic helix–loop–helix transcription factor ID1 as an IRE1α RNase target. Further, we demonstrate that *Id1* degradation by IRE1α is essential for HRas-induced premature senescence. Together, our studies point to IRE1α as an important node for posttranscriptional regulation of the early Ras phenotype that is dependent on both oncogenic signaling as well as stress signals imparted by the tumor microenvironment and could be an important mechanism driving escape from Ras-induced senescence.

oncogene-induced senescence | ER stress | IRE1α | Ras | ID1

Inositol requiring enzyme 1α (IRE1α) is an endoplasmic reticulum (ER) transmembrane kinase/endoribonuclease (RNase) that functions as a major driver of the unfolded protein response (UPR). Accumulation of unfolded proteins causes IRE1α to undergo dimerization and autophosphorylation, which activates its RNase domain (1). A major target of the RNase is X-box binding protein 1 (*Xbp1*) mRNA, which is critical for induction of genes important in resolution of ER stress (2, 3). IRE1α-induced cleavage at specific sites removes an internal 26-nt intron followed by splicing of the *Xbp1* mRNA to generate a new reading frame encoding the active transcription factor, XBP1s (2). IRE1α can target other mRNAs for degradation in a process called regulated IRE1α-dependent decay (RIDD), which functions to reduce levels of mRNAs encoding proteins processed through the ER (4, 5), although transcripts encoding cytosolic or nuclear proteins are also RIDD targets (6, 7). More recent studies implicate RIDD activation in apoptosis following unremitting ER stress (5, 8, 9).

Activation of the UPR occurs frequently in human solid cancers and is an adaptive response to environmental and metabolic stress or aberrant protein expression (10). XBP1 is overexpressed in human cancers and is associated with aggressive disease and the malignant phenotype (11–14). Functions of RIDD are poorly understood, but in a glioblastoma model, RIDD targeting of PER1 mRNA enhances tumorigenesis, while targeting of SPARC reduces tumor migration and invasiveness (6, 15). How these two IRE1α RNase outputs function in early stages of cancer is not known. Expression of a Ras oncogene in primary human or mouse cells causes premature senescence, a well-characterized mechanism of tumor suppression (16–18). While a previous study showed that $HRas^{G12V}$-driven ER stress was linked to senescence of melanocytes (19), we found that ER stress opposes senescence in epidermal keratinocytes (20). Here, we show that the IRE1α pathway is a critical target of HRas signaling in keratinocytes but that the two outputs of the IRE1α RNase have opposing effects on cell proliferation and premature senescence. While ER stress and IRE1α-mediated *Xbp1* splicing enhance HRas-induced proliferation, IRE1α-mediated RIDD promotes premature senescence through degradation of prooncogenic factor *Id1* mRNA. Both ER stress and HRas-driven IRE1α overexpression influence *Xbp1* splicing and RIDD, revealing a complex role of IRE1α signaling in cancer.

Results

ER Stress and IRE1α-Mediated *Xbp1* Splicing Are Required for Maximum HRas-Induced Proliferation. We introduced oncogenic v-Ha-Ras (HRas) into primary mouse keratinocytes using a high-titer retrovirus (17) that causes an initial hyperproliferative phenotype

Significance

Inositol requiring enzyme 1α (IRE1α) is a mediator of the unfolded protein response that determines adaptation or cell death in response to endoplasmic reticulum (ER) stress through its distinct endoribonuclease (RNase) activities of *Xbp1* splicing and mRNA decay, but its role in cancer is poorly understood. In normal epithelial cells, we find that Ras oncogene-induced proliferation and senescence are directly linked to IRE1α activation. Proliferation requires *Xbp1* splicing and ER stress, while IRE1α-catalyzed degradation of *Id1* mRNA drives senescence in conjunction with reduced ER stress. Thus, we propose that oncogene and ER stress regulation of the IRE1α RNase dictates tumor promotion or suppression in Ras-driven cancers.

Author contributions: N.B. and A.B.G. designed research; N.B., J.S., A.B.C.-L., C.L.J., K.J.B., and M.A.P. performed research; J.S. contributed new reagents/analytic tools; N.B. and A.B.G. analyzed data; and N.B. and A.B.G. wrote the paper.

The authors declare no conflict of interest.

This article is a PNAS Direct Submission.

Data deposition: The microarray dataset reported in this paper has been deposited in the Gene Expression Omnibus (GEO) database, https://www.ncbi.nlm.nih.gov/geo (accession no. GSE70899).

[1]Present address: Division of Pharmacology and Toxicology, College of Pharmacy, The University of Texas at Austin, Austin, TX 78712.

[2]Present address: Department of Hematology, Children's Hospital of Philadelphia, Philadelphia, PA 19104.

[3]To whom correspondence should be addressed. Email: abg11@psu.edu.

This article contains supporting information online at www.pnas.org/lookup/suppl/doi:10.1073/pnas.1701757114/-/DCSupplemental.

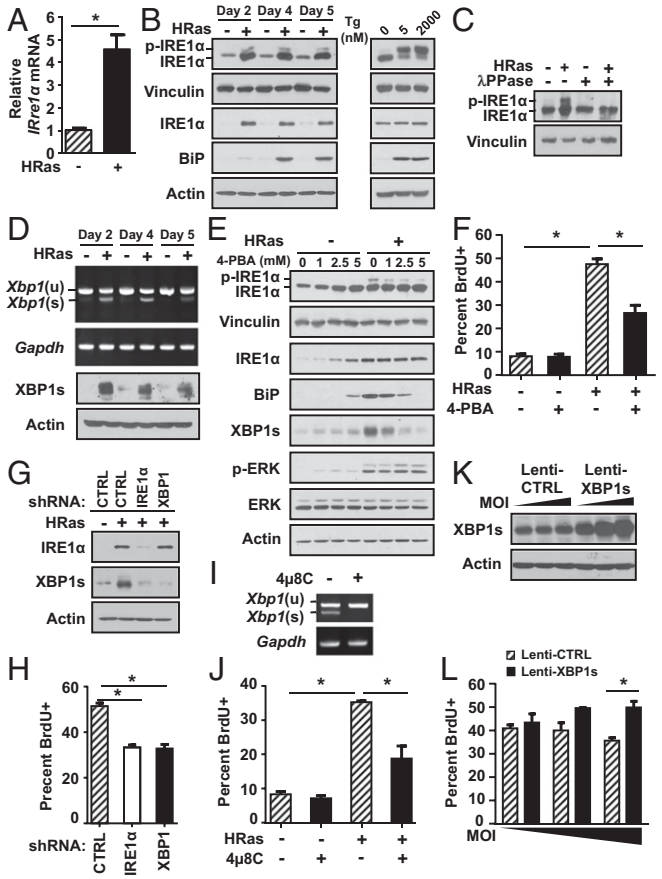

Fig. 1. ER stress and IRE1α-mediated *Xbp1* splicing are required for HRas-induced proliferation. (*A*) *Ire1α* mRNA expression in primary and HRas keratinocytes 5 d after transduction. (*B*, *Left*) Immunoblots of phosphorylated IRE1α and total IRE1α in primary and HRas keratinocytes at indicated time points. (*B*, *Right*) For comparison, primary keratinocytes were treated with the ER stress inducer thapsigargin for 6 h at 5 nM and 2,000 nM. (*C*) Immunoblot of phosphorylated IRE1α in primary and HRas keratinocytes after treatment of cell lysates with λ-phosphatase. (*D*) *Xbp1*(*s*) and *Xbp1*(*u*) mRNA expression (*Top*) and immunoblot of XBP1s (*Bottom*) of primary and HRas keratinocytes at indicated time points. (*E*) Immunoblots of primary and HRas keratinocytes treated with increasing doses of 4-PBA for 24 h. (*F*) Percent proliferation of HRas keratinocytes after treatment with 2.5 mM 4-PBA for 24 h. Immunoblot analysis (*G*) and percent proliferation of HRas keratinocytes cotransduced with lentiviral shRNA specific for IRE1α or XBP1 or control (CTRL) shRNA 5 d after transduction (*H*) are shown. *Xbp1*(*s*) and *Xbp1*(*u*) mRNA expression (*I*) and percent proliferation of HRas keratinocytes treated with 4μ8C (20 μM) for 24 h and examined 4 d after transduction (*J*) are shown. XBP1(*s*) immunoblot (*K*) and percent proliferation of HRas keratinocytes cotransduced with 2.5, 5, and 10 multiplicity of infection (MOI) of CTRL or pWPI-*Xbp1s* lentivirus (*L*) are shown. In *A*, *F*, *H*, *J*, and *L*, data represent mean ± SEM ($n = 3$). *$P < 0.05$ as determined by a Student's *t* test.

in vitro and benign squamous lesions in vivo (21). HRas induced *Ire1α* mRNA (Fig. 1*A*), total IRE1α protein levels (Fig. 1*B*, *Left*), and phosphorylated IRE1α which was detected using Phos-Tag SDS/PAGE (22) and validated with λ-phosphatase treatment (Fig. 1*C*). However, the level of phosphorylated IRE1α was much lower than the level of primary keratinocytes treated with the ER stress inducer thapsigargin at nanomolar concentrations (Fig. 1*B*, *Right*). IRE1α-mediated *Xbp1* splicing increased in HRas keratinocytes (Fig. 1*D*), indicating activation of the IRE1α RNase, and this was not solely an in vitro response, as we detected increased *Ire1α* mRNA and *Xbp1* splicing in 7,12-dimethylbenz[a] anthracene/12-O-tetradecanoylphorbol-13-acetate (DMBA/TPA)–generated benign and malignant mouse cutaneous squamous tumors (Fig. S1*A*) and in tumors from a skin-targeted inducible human Ras^{G12V} model (Fig. S1*B*).

We next examined if ER stress was responsible for IRE1α activation in HRas keratinocytes. HRas caused a marked increase in ER size (Fig. S2*A*) and an increase in the UPR target genes BiP, *Ero1l*, *Crt*, *Pdia4*, and *Pdia5* (Fig. 1*B* and Fig. S2*B*), indicating active ER stress. HRas keratinocytes exhibited no difference in viability compared with primary keratinocytes, suggesting active ER stress was adaptive and not apoptotic (Fig. S2*C*). Treatment with 4-phenyl butyric acid (4-PBA), a molecular chaperone that dampens ER stress by decreasing unfolded proteins in the ER lumen (23), caused a dose-dependent decrease in IRE1α phosphorylation but had no effect on HRas induction of total IRE1α or HRas-activated mitogen-activated protein kinase kinase 1 (MEK)–extracellular signal-regulated kinase (ERK) signaling (Fig. 1*E*). However, 4-PBA treatment reduced *Xbp1* splicing and BiP protein levels, indicating that *Xbp1* splicing through IRE1α is dependent on ER stress. In contrast, inhibition of MEK-ERK signaling with UO126 blocked induction of *Ire1α* mRNA and total IRE1α protein levels and reduced *Xbp1* splicing (Fig. S2 *D* and *E*). Thus, IRE1α expression is regulated by this Ras effector pathway independent of ER stress. Treatment with 4-PBA reduced proliferation of HRas keratinocytes, suggesting that the increased burden of unfolded proteins and subsequent IRE1α activation is linked to elevated proliferation (Fig. 1*F*). To directly test if activation of the IRE1α pathway was critical for HRas-induced proliferation, we used lentiviral shRNA to knock down either IRE1α or XBP1 in HRas keratinocytes. Both shRNAs caused a significant and similar decrease in *Xbp1* splicing (Fig. 1*G*) and in proliferation compared with nontarget control shRNA (Fig. 1*H*). Similarly, a 24-h treatment with a noncytotoxic dose of the IRE1α RNase inhibitor 4μ8C (24) completely blocked *Xbp1* splicing and reduced proliferation (Fig. 1 *I* and *J*), while cotransduction of HRas keratinocytes with a lentivirus expressing XBP1s (Fig. 1*K*) caused an increase in proliferation (Fig. 1*L*).

While *Xbp1* splicing increased in response to HRas, there was a decrease in phosphorylation of JNK and p38 kinases at 2 d and 4 d after transduction (Fig. S3*A*), and expression of HRas using primary K14rTA × tetOH-Ras^{G12V} keratinocytes with increasing doses of doxycycline showed reduced phosphorylation of JNK and downstream target c-JUN within 24 h (Fig. S3*B*). In contrast, ER stress induction with thapsigargin caused phosphorylation of JNK, previously shown to be IRE1α-dependent (25), and phosphorylation of c-JUN (Fig. S3*C*). Together, these results indicate that JNK pathway activation is not a significant response to HRas in keratinocytes. We also examined other UPR pathways that are activated under ER stress conditions. HRas did not cause increased phosphorylation of protein kinase R-like endoplasmic reticulum kinase (PERK) and total PERK protein levels or its downstream target eIF2α (Fig. S3*D*), and while *Atf4* mRNA increased, there was no increase in *Chop* mRNA, indicating lack of activation of the PERK arm of the UPR (Fig. S3*E*). Although we were unable to adequately detect activating transcription factor 6 (ATF6), knockdown of IRE1α or XBP1 did not block induction of UPR target genes (Fig. S3*F*), suggesting a potential relevance of ATF6 in the response to HRas. Nevertheless, our results show that oncogenic HRas promotes IRE1α activation and *Xbp1* splicing through the coordinate action of ER stress and MEK-ERK signaling and that this arm of the UPR pathway is required for maximal HRas-driven proliferation.

IRE1α Promotes HRas-Induced Senescence Under Reduced ER Stress. We next sought to understand the role of ER stress and IRE1α during premature senescence. Following the initial proliferative response, keratinocytes expressing oncogenic HRas undergo premature senescence after 7–10 d, characterized by growth arrest (Fig. S4*A*) and increased senescence-associated β-galactosidase

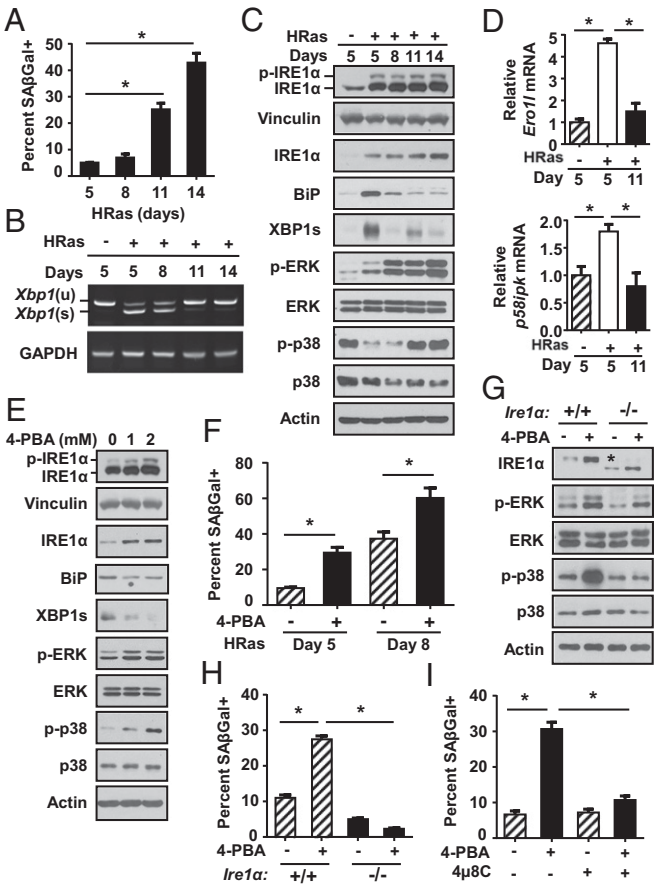

Fig. 2. Reduced ER stress accelerates HRas-induced senescence dependent on IRE1α. (*A*) Percent senescence at indicated time points after HRas transduction. *Xbp1*(*s*) and *Xbp1*(*u*) mRNA expression (*B*) and immunoblots of IRE1α and Ras pathway proteins at indicated time points after HRas transduction (*C*) are shown. (*D*) qPCR analysis of *Ero1l* and *p58ipk* at indicated time points after HRas transduction. (*E*) Immunoblots of HRas keratinocytes on day 5 posttransduction after treatment with 4-PBA for 3 d. (*F*) Percent senescence of HRas keratinocytes at indicated time points after treatment with 4-PBA (2 mM) for 3 and 6 d. Immunoblot analysis (*G*) and percent senescent cells after treatment of $Ire1\alpha^{+/+}$ and $Ire1\alpha^{-/-}$ HRas keratinocytes with 4-PBA (2 mM) for 3 d and examined 5 d after transduction (*H*) are shown. The asterisk in *G* represents truncated inactive IRE1α generated by Cre deletion. (*I*) Percent senescence of HRas keratinocytes after treatment with 4-PBA (2 mM), 4μ8C (20 μM), or in combination for 3 d and examined 5 d after transduction. In *A*, *D*, *F*, *H*, and *I*, data represent mean ± SEM ($n = 3$). *$P < 0.05$ as determined by a Student's *t* test.

(SA–β-gal) activity (17, 26) (Fig. 2*A*). These cells were heavily vacuolated (Fig. S4 *B* and *C*) and had high levels of MAPK pathway proteins, such as phosphorylated p38 and ERK1/2 kinases, which paradoxically promote senescence (27–29) (Fig. 2*C*). Senescence occurred in parallel with reduced expression of several markers of ER stress, including UPR target genes *Ero1l* and *p58ipk* (Fig. 2*D*), *Xbp1* splicing, and BiP (Fig. 2 *B* and *C*). In addition, ER-Tracker Green and protein disulfide isomerase staining (Fig. S4*D*) showed reduced ER content in HRas keratinocytes undergoing senescence compared with earlier time points (Fig. S4 *E* and *F*), further suggesting dampening of the ER stress response. In contrast, total IRE1α protein levels and, to a lesser extent, phosphorylated IRE1α increased in cells undergoing senescence, paralleling increased MAPK signaling (Fig. 2*C*). Reduction of ER stress with prolonged 4-PBA treatment led to decreased *Xbp1* splicing and BiP protein levels as expected, but also increased total and phosphorylated IRE1α (Fig. 2*E*) and increased senescence (Fig. 2*F*). Given that IRE1α can function with no overt signs of an ER stress response (1), we hypothesized that despite reduced *Xbp1* splicing and other markers of ER stress, increased IRE1α may promote senescence. To test this, we introduced HRas into primary $Ire1\alpha^{fl/fl}$ keratinocytes, deleted IRE1α with a Cre adenovirus, and measured accelerated senescence induced by 4-PBA (Fig. 2*G*). *Ire1α* deletion completely blocked the increase in SA–β-gal–positive cells (Fig. 2*H*) and significantly decreased p38 and ERK1/2 kinase activation caused by 4-PBA (Fig. 2*G*). Similar results were observed with the IRE1α RNase inhibitor 4μ8C (Fig. 2*I*), although some cytotoxicity was observed after prolonged treatment. These results indicate that in keratinocytes expressing oncogenic HRas, reduced ER stress accelerates premature senescence dependent on an intact IRE1α RNase pathway.

Opposing Roles of IRE1α and XBP1 During HRas-Induced Senescence. To further examine the role of IRE1α in the senescence response, we compared effects of prolonged IRE1α or XBP1 knockdown in HRas keratinocytes. While short-term IRE1α knockdown reduced proliferation during the initial proliferative phase as expected, long-term IRE1α knockdown blocked induction of senescence instead, causing sustained hyperproliferation (Fig. 3 *A* and *B*). In contrast, XBP1 knockdown accelerated growth arrest and senescence (Fig. 3 *A* and *B*). Consistent with accelerated senescence, XBP1 knockdown caused an early and sustained increase in phosphorylated p38 and ERK1/2 kinases, while in cells with IRE1α knockdown and sustained proliferation, these were reduced (Fig. 3*C*).

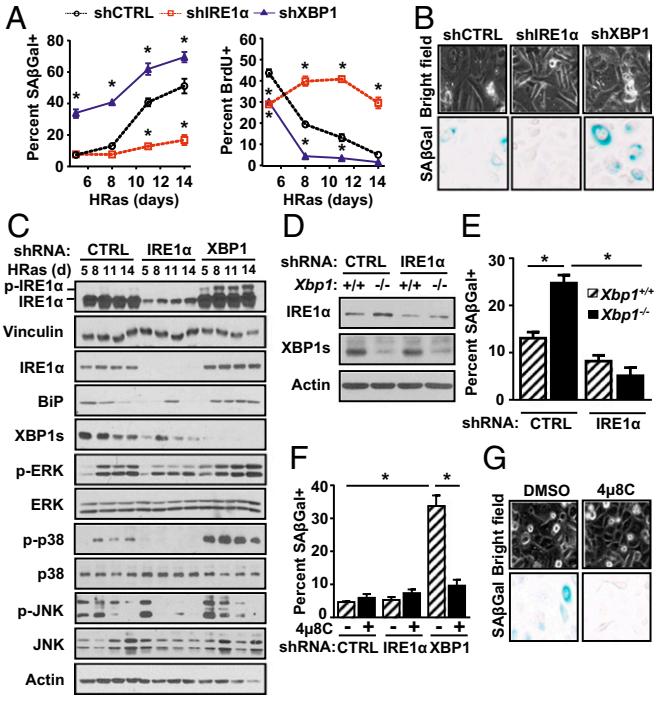

Fig. 3. IRE1α RNase promotes senescence in the absence of mRNA cleavage target *Xbp1*. (*A*) Percent senescence (*Left*) and percent proliferation (*Right*) of HRas keratinocytes cotransduced with lentiviral shRNA specific for IRE1α, XBP1, or control (CTRL) shRNA at indicated time points after transduction. (*B*) Representative images of cellular vacuolization (*Top*) and SA–β-gal staining (*Bottom*) of groups in *A*. (Original magnification: 20×.) (*C*) Immunoblot analysis of groups in *A*. Immunoblots (*D*) and percent senescence of $Xbp1^{+/+}$ and $Xbp1^{-/-}$ HRas keratinocytes cotransduced with lentiviral shRNA specific for IRE1α or CTRL shRNA and examined 5 d after transduction (*E*) are shown. (*F*) Percent senescence on day 5 posttransduction of HRas keratinocytes cotransduced with lentiviral shRNA specific for IRE1α, XBP1, or CTRL shRNA and treated with 4μ8C (20 μM) for 3 d. (*G*) Representative images of cellular vacuolization (*Top*) and SA–β-gal staining (*Bottom*) of groups in *F*. (Original magnification: 20×.) In *A*, *E*, and *F*, data represent mean ± SEM ($n = 3$). *$P < 0.05$ as determined by a Student's *t* test.

This increase was specific for p38 and ERK 1/2 kinases as phosphorylated JNK levels decreased independent of specific knockdown (Fig. 3*C*). XBP1 knockdown also increased phosphorylated and total IRE1α protein levels (Fig. 3*C*), as previously shown in other physiological models of XBP1 deletion (9, 30, 31). Blockade of MEK-ERK signaling in these cells significantly suppressed the accelerated senescence response (Fig. S5*A*), as well as phosphorylated IRE1α and total IRE1α protein levels (Fig. S5*B*).

To test if accelerated senescence caused by XBP1 knockdown was driven by IRE1α hyperactivation similar to 4-PBA, we deleted *Xbp1* with Cre adenovirus in primary *Xbp1*$^{fl/fl}$ keratinocytes, followed by shRNA knockdown of IRE1α. *Xbp1* deletion accelerated senescence of HRas keratinocytes as expected but was blocked by IRE1α knockdown (Fig. 3 *D* and *E*). Similarly, 4μ8C treatment also blocked the accelerated senescence response (Fig. 3 *F* and *G*). In contrast, treatment of primary keratinocytes with a cell-permeable JNK inhibitor that blocked thapsigargin-induced c-JUN phosphorylation (Fig. S5*C*) and reduced basal levels of phosphorylated c-JUN in both control and *Xbp1*-deleted HRas keratinocytes (Fig. S5 *D* and *E*) had no impact on basal and accelerated senescence in either genotype (Fig. S5*F*). Taken together, these results implicate IRE1α RNase activity independent of XBP1 and JNK signaling in HRas-induced senescence.

Cleavage of *Id1* mRNA by IRE1α Mediates HRas-Induced Senescence. Degradation of cellular mRNAs through RIDD is a second activity of the IRE1α RNase that is essential for physiological processes, such as lipid metabolism, pancreatic β-cell homeostasis, and innate and adaptive immunity (9, 30, 32, 33). We determined that two previously characterized RIDD mRNA targets, peripheral myelin protein 22 (*Pmp22*) and heparan–α-glucosaminide *N*-acetyltransferase (*Hgsnat*) (4, 24), were down-regulated by HRas in an IRE1α-dependent manner (Fig. S6 *A*–*C*), showing that both *Xbp1* splicing and RIDD functions of IRE1α are coordinately activated by oncogenic HRas. Using a microarray screen of HRas keratinocytes with IRE1α or XBP1 knockdown to identify specific RIDD targets that may be critical for induction of the senescence response (RIDD target criteria are discussed in *Materials and Methods*), we found 73 mRNAs whose down-regulation by oncogenic HRas was IRE1α-dependent, including RIDD target *Pmp22* (Fig. S6*D* and Table S1). Many of these targets exhibited enhanced down-regulation in XBP1 knockdown cells, paralleling increased IRE1α activation (Fig. S6*D* and Table S1). Annotation of these mRNAs showed that 43% encoded secretory pathway proteins, while 57% encoded cytosolic or nuclear proteins (Fig. S7*A*). Top targets included the secretory proteins insulin-like growth factor binding protein 2 (*Igfbp2*) and matrix metalloproteinase inhibitor (*Timp3*). IRE1α-dependent down-regulation of these two mRNAs was confirmed by shRNA knockdown in HRas keratinocytes (Fig. S7*B*) and by treatment with 4μ8C for 24 h (Fig. S7*C*). Bioinformatic analysis showed that 38 of the putative RIDD mRNA targets, including *Igfbp2* and *Timp3*, were strongly associated with cancer progression (Fig. S7*D*). Sixty-three percent of these targets were linked to cell growth/proliferation, while 37% were linked to the metastatic phenotype (Fig. S7*E*), suggesting that IRE1α signaling may promote senescence in HRas keratinocytes by down-regulating genes that are prooncogenic. Pathway analysis revealed that ERK1/2 was a major node of regulation for these genes (Fig. S7*F*), consistent with effects of U0126 on IRE1α activation and signaling during proliferation and senescence (Fig. 4 and Fig. S3).

Of the putative RIDD targets identified, a notable group down-regulated by IRE1α comprised three members of the Id family, *Id1*, *Id2*, and *Id3* (Fig. S6*D* and Table S1), which are basic helix–loop–helix transcription factors linked to development and cancer (34). In particular, ID1 overexpression is strongly linked to escape from replicative senescence and bypass of Ras-induced senescence (35–37), making it a likely candidate for mediating the senescence block associated with IRE1α depletion. We confirmed IRE1α-dependent

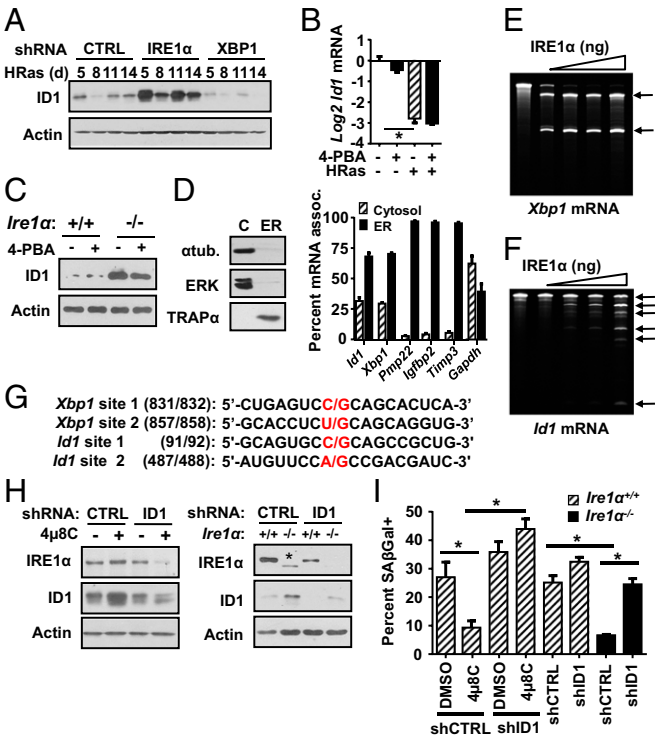

Fig. 4. IRE1α mediates HRas-induced senescence through cleavage of *Id1* mRNA. (*A*) Immunoblots of HRas keratinocytes cotransduced with shRNA specific for IRE1α, XBP1, or control (CTRL) shRNA at indicated time points after transduction. (*B*) qPCR analysis of day 5 HRas keratinocytes treated with 4-PBA (2.5 mM) 24 h before harvest. (*C*) Immunoblot of ID1 expression in IRE1α$^{+/+}$ or IRE1α$^{-/-}$ day 5 HRas keratinocytes treated with 4-PBA (2 mM) for 3 d before harvest. (*D*) Immunoblots of cytosolic and ER resident proteins (*Left*) and qPCR analysis of IRE1α mRNA targets (*Right*) from cytosolic and ER fractions isolated from primary keratinocytes by sequential digitonin fractionation. Each mRNA was normalized to 18S, which had an equal distribution in both fractions. Cleavage assay of in vitro-transcribed *Xbp1* (*E*) and *Id1* (*F*) mRNA with increasing amounts of purified human IRE1α cytosolic region (amino acids 465–977). Black arrows indicate cleavage products. (*G*) Sequence of *Id1* mRNA cleavage sites identified by 5′ RACE. *Xbp1* mRNA cleavage sites are shown for comparison. (*H*) Immunoblot analysis of HRas keratinocytes cotransduced with lentiviral shRNA specific for ID1 or CTRL shRNA and treated with 4μ8C (20 μM) for 6 d (*Left*) or *Ire1α*$^{+/+}$ and *Ire1α*$^{-/-}$ HRas keratinocytes cotransduced with lentiviral shRNA specific for ID1 or CTRL shRNA (*Right*), with both examined 8 d after transduction. The asterisk represents truncated inactive IRE1α generated by Cre deletion. (*I*) Percent senescence of groups described in *H*, *B*, *D*, and *I* represent mean ± SEM ($n = 3$). *$P < 0.05$ as determined by a Student's *t* test.

down-regulation of *Id1* mRNA levels and other family members by shRNA knockdown in HRas keratinocytes (Fig. S8*A*) and with 4μ8C treatment for 24 h (Fig. S8*B*). Additionally, in transgenic keratinocytes expressing a doxycycline-inducible human HRAS^{G12V} allele, treatment with 4μ8C reversed down-regulation of *Id1* mRNA and ID1 protein levels (Fig. S8 *C* and *D*). IRE1α knockdown induced ID1 protein levels at all time points examined, paralleling blocked senescence, while XBP1 knockdown enhanced ID1 down-regulation (Fig. 4*A*). Furthermore, HRas mediated down-regulation of *Id1* mRNA was not altered by 4-PBA treatment (Fig. 4*B*), and 4-PBA did not block increased ID1 protein levels when IRE1α was deleted in HRas-transduced primary *Ire1α*$^{fl/fl}$ keratinocytes (Fig. 4*C*). These results link the phenotype of senescence escape under conditions of reduced ER stress in IRE1α-deleted cells to sustained ID1 expression.

We next determined if IRE1α regulates *Id1* mRNA levels through a mechanism dependent on direct cleavage. Even though *Id1* mRNA is thought to be predominately localized in the cytosol, transcriptomic analysis previously showed enrichment of *Id1*

mRNA in the ER membrane fraction of mammalian cells (38). To confirm this, we used digitonin fractionation to separate cytosolic and ER-associated mRNAs (39). As expected α-tubulin and ERK1/2 proteins were enriched in the cytosolic fraction, and the ER membrane protein TRAPα was enriched in the ER fraction (Fig. 4*D*). In agreement with published results, the majority of *Id1* mRNA was enriched with the ER fraction (70%) and not the cytosol, similar to *Xbp1* mRNA (Fig. 4*D*), while 95% of the mRNAs for *Igfbp2*, *Timp3*, and *Pmp22* were enriched in the ER fraction as expected for proteins of the secretory pathway. In contrast, *Gapdh* mRNA had a near-equal distribution in the cytosolic and ER fractions (Fig. 4*D*).

To directly demonstrate cleavage by IRE1α, we incubated in vitro-transcribed *Id1* mRNA with recombinant IRE1α protein. As expected, IRE1α cleaved *Xbp1* mRNA into two fragments of the expected sizes (Fig. 4*E*). Importantly, in vitro-transcribed *Id1* mRNA was also cleaved by IRE1α, producing two major cleavage fragments and several minor fragments (Fig. 4*F*). Using 5′ RACE, we identified two cleavage sites in *Id1* mRNA that are similar in sequence to the known *Xbp1* mRNA cleavage sites (Fig. 4*G*), form stem–loop structures similar to *Xbp1* mRNA and other IRE1α cleavage targets (40) (Fig. S9*A*), and produce predicted fragments consistent in size with the two major fragments identified by the cleavage assay. When purified total RNA from primary keratinocytes was incubated with recombinant IRE1α, and subsequent cDNA was amplified using primers that spanned these predicted IRE1α cleavage sites (Fig. S9*B*), *Id1* mRNA was significantly reduced compared with primers that spanned a region lacking these cleavage sites (Fig. S9*C*). Similar reduced amplification of *Xbp1* mRNA occurred with primers that spanned known cleavage sites, but not with noncleavage site primers (Fig. S9*D*). Thus, IRE1α can promote sequence-specific cleavage of both in vitro-transcribed and endogenous *Id1* mRNA.

To determine if *Id1* mRNA cleavage by IRE1α was critical for HRas-induced senescence, we measured SA–β-gal–positive cells in HRas-transduced *Ire1α*$^{fl/fl}$ keratinocytes with ID1 knockdown and either genetic or pharmacological inactivation of IRE1α. Fig. 4*H* shows that 4μ8C treatment or IRE1α deletion increased ID1 protein levels in HRas keratinocytes transduced with nontarget control shRNA and significantly suppressed senescence (Fig. 4*I*). In contrast, ID1 knockdown (Fig. 4*H*) completely reversed the suppressive effect of 4μ8c or *Ire1α* ablation on senescence (Fig. 4*I*). Collectively, these data support the conclusion that *Id1* mRNA is a direct cleavage target of IRE1α and that its degradation by IRE1α is required for HRas-induced senescence.

Discussion

The UPR can generate both adaptive and apoptotic responses, leading to the paradigm that levels of ER stress and distinct UPR outputs determine the balance between cell death and survival during cancer progression (10). Our results expand understanding of the bifunctional nature of the IRE1α RNase in cell fate regulation linked to the earliest stage of cancer. We show that oncogenic HRas induces and activates the IRE1α RNase in primary epidermal keratinocytes through the MEK-ERK pathway and that IRE1α and *Xbp1* splicing are elevated in mouse cutaneous squamous tumors. In contrast to primary melanocytes, where HRas engages multiple UPR pathways (19), the lack of changes in PERK and PERK targets, such as p-eIF2α and CHOP, suggests minimal activation of this pathway in keratinocytes. Similarly, the absence of JNK activation and low levels of IRE1α phosphorylation suggest that the activation of IRE1α by HRas is distinct from other ER stress activators. Since knockdown of IRE1α or XBP1 did not reduce expression of many UPR/ER stress target genes induced by HRas, we cannot rule out a possible role for ATF6, although difficulties in detecting expression and activation of ATF6 prevented direct analysis. While it will be important to determine if ATF6 has overlapping or distinct roles in regulating responses to oncogenic HRas, our data clearly show the importance of the IRE1α pathway in proliferation and senescence. IRE1α activation and *Xbp1* splicing were proproliferative in HRas keratinocytes and dependent on ER stress for this response. HRas-induced ER stress linked to proliferation was characterized by a rapid expansion of the ER membrane, increased *Xbp1* splicing, and up-regulation of several UPR/ER stress target genes. However, during senescence, levels of BiP, *p58ipk*, and *Ero1L*, as well as *Xbp1* splicing and ER content, were reduced. This adaptive/proproliferative role of ER stress and *Xbp1* splicing is consistent with the tumor-promoting and antisenescence role of chemical ER stress activators in the skin (20, 41) and with association of *Xbp1* splicing with cancer progression in several human and mouse cancer models (2).

Unexpectedly, modulating ER stress levels or perturbing *Xbp1* splicing revealed an alternate RNase output of the IRE1α pathway that is essential for the senescence response. Reduction of ER stress with the chemical chaperone 4-PBA or shRNA knockdown/genetic deletion of XBP1 drastically accelerated the HRas-induced senescence response. Under both conditions, IRE1α phosphorylation and total IRE1α further increased, representing a "hyperactive state" that reflects removal of a negative feedback loop similar to previous studies using targeted XBP1 null mouse models (30, 31). However, due to the nonspecific nature of Phos-tag analysis, it is unclear if this increased phosphorylation is on ser724 or ser726 in the activation loop, which are both normally phosphorylated in response to ER stress, or on additional sites that could modulate IRE1α activity (42). Nevertheless, genetic ablation, shRNA knockdown, or pharmacological inhibition of hyperactive IRE1α blocked senescence and revealed a previously uncharacterized tumor suppressor role for IRE1α.

Degradation of specific mRNA targets by the IRE1α RNase has been linked to diverse normal cellular and metabolic functions (9, 30, 31), as well as to pathological states such as apoptosis caused by prolonged ER stress (43, 44), and to tumor invasiveness and proliferation (6, 15). Thus, the set of mRNAs that can be degradation targets is likely to be dependent on the cell type and stress environment. Of the putative RIDD mRNA targets identified, *Id1* is most notable due to its well-characterized antisenescence/prooncogenic function in cancer (35, 36, 45). Based on several lines of evidence, including preferential association of *Id1* mRNA to the ER; identification of IRE1α RNase consensus sites; in vitro degradation of *Id1* mRNA by purified IRE1α at these sites; and reversal of *Id1* mRNA down-regulation by IRE1α knockdown, genetic ablation, or pharmacological RNase inactivation, we conclude that *Id1* mRNA is a direct target of the IRE1α RNase. Although other targets and mechanisms may contribute, degradation of *Id1* mRNA is critically important in driving senescence as shRNA knockdown reverses reduced senescence due to IRE1α inhibition. Together with previous results showing defective ER stress-induced RIDD in benign pancreatic insulinoma INS-1 cells overexpressing human cancer-associated mutant IRE1α proteins (46), it is clear that alteration of RIDD activity is likely to be important in cancer progression. We propose that oncogenic Ras induces a stress response in primary keratinocytes, in part, through MAPK activation that causes IRE1α up-regulation and activation of both outputs of its RNase (Fig. S9*E*). Under conditions of ER stress, the proliferative and adaptive functions of *Xbp1* splicing predominate, but with time and reduced ER stress, *Xbp1* splicing is reduced and prosenescent RIDD targets, such as degradation of *Id1* mRNA, drive Ras keratinocytes into senescence. Senescence is further amplified due to increased phosphorylation of ERK1/2, which drives IRE1α hyperactivation and generates a positive feedback loop under reduced ER stress. However, the exact mechanism by which elevated IRE1α under conditions of normally occurring or 4-PBA–induced ER stress reduction could differentially affect *Xbp1* splicing and RIDD is unclear.

An emerging model of IRE1α activation is initial formation of IRE1α monomers into dimers and autophosphorylation preferentially linked to *Xbp1* mRNA cleavage and splicing, with increasing ER stress levels causing formation of high-order

oligomers allowing for relaxed mRNA specificity and degradation of many mRNA targets through RIDD (5, 46). This allows for the adaptive functions of IRE1α mediated through *Xbp1* splicing to be separated temporally and quantitatively from the cell death function of RIDD that occurs in response to chemical ER stress. Although speculative and requiring further study, it is possible that similar changes in IRE1α dimer/oligomeric states occur during the response to oncogenic HRas. Taken together, these studies point to IRE1α as an important node for post-transcriptional regulation of the cancer cell phenotype that is dependent on both oncogenic signaling and stress signals imparted by the tumor microenvironment.

Materials and Methods

Antibodies, reagents, and isolation of newborn primary keratinocytes used in this study are described in *SI Materials and Methods*. All experiments were processed according to standard protocols. Plasmids, viral production and infection, real-time RT-PCR, immunoblot analysis, SA–β-gal staining, 5-bromo-2′-deoxyuridine incorporation, and in vitro RNA cleavage assays, for example, are described in detail in *SI Materials and Methods*. The microarray dataset was deposited in the Gene Expression Omnibus database (accession no. GSE70899). All animals for tumor studies or generation of primary keratinocyte cultures were housed and treated according to protocols approved by the Pennsylvania State University Institutional Animal Care and Use Committee.

ACKNOWLEDGMENTS. We thank the Huck Institutes of Life Sciences Flow Cytometry Facility and Penn State Genomics Core Facility and the Penn State Animal Research Program and animal caretakers for their help, and we thank Dr. Laurie Glimcher and Dr. Ann-Hwee Lee for *Ire1a*$^{fl/fl}$ and *Xbp1*$^{fl/fl}$ mice. We also thank Dr. Bokai Zhu and Dr. Jeffrey Peters and The Pennsylvania State University for helpful discussions and sharing of results during early stages of this project. This work was supported by funds from the Department of Veterinary and Biomedical Sciences, the Penn State Institute for Energy and the Environment, and the Elsa U. Pardee Foundation, and by NIH Grant 1 R01 CA197942 (to A.B.G.).

1. Hetz C, Martinon F, Rodriguez D, Glimcher LH (2011) The unfolded protein response: Integrating stress signals through the stress sensor IRE1α. *Physiol Rev* 91:1219–1243.
2. Glimcher LH (2010) XBP1: The last two decades. *Ann Rheum Dis* 69(Suppl 1):i67–i71.
3. Lee AH, Iwakoshi NN, Glimcher LH (2003) XBP-1 regulates a subset of endoplasmic reticulum resident chaperone genes in the unfolded protein response. *Mol Cell Biol* 23:7448–7459.
4. Hollien J, et al. (2009) Regulated Ire1-dependent decay of messenger RNAs in mammalian cells. *J Cell Biol* 186:323–331.
5. Han D, et al. (2009) IRE1alpha kinase activation modes control alternate endoribonuclease outputs to determine divergent cell fates. *Cell* 138:562–575.
6. Pluquet O, et al. (2013) Posttranscriptional regulation of PER1 underlies the oncogenic function of IREα. *Cancer Res* 73:4732–4743.
7. Moore KA, Plant JJ, Gaddam D, Craft J, Hollien J (2013) Regulation of sumo mRNA during endoplasmic reticulum stress. *PLoS One* 8:e75723.
8. Li H, Korennykh AV, Behrman SL, Walter P (2010) Mammalian endoplasmic reticulum stress sensor IRE1 signals by dynamic clustering. *Proc Natl Acad Sci USA* 107:16113–16118.
9. Lee AH, Heidtman K, Hotamisligil GS, Glimcher LH (2011) Dual and opposing roles of the unfolded protein response regulated by IRE1alpha and XBP1 in proinsulin processing and insulin secretion. *Proc Natl Acad Sci USA* 108:8885–8890.
10. Wang M, Kaufman RJ (2014) The impact of the endoplasmic reticulum protein-folding environment on cancer development. *Nat Rev Cancer* 14:581–597.
11. Fujimoto T, et al. (2003) Upregulation and overexpression of human X-box binding protein 1 (hXBP-1) gene in primary breast cancers. *Breast Cancer* 10:301–306.
12. Fujimoto T, et al. (2007) Overexpression of human X-box binding protein 1 (XBP-1) in colorectal adenomas and adenocarcinomas. *Anticancer Res* 27:127–131.
13. Romero-Ramirez L, et al. (2004) XBP1 is essential for survival under hypoxic conditions and is required for tumor growth. *Cancer Res* 64:5943–5947.
14. Carrasco DR, et al. (2007) The differentiation and stress response factor XBP-1 drives multiple myeloma pathogenesis. *Cancer Cell* 11:349–360.
15. Dejeans N, et al. (2012) Autocrine control of glioma cells adhesion and migration through IRE1α-mediated cleavage of SPARC mRNA. *J Cell Sci* 125:4278–4287.
16. Serrano M, Lin AW, McCurrach ME, Beach D, Lowe SW (1997) Oncogenic ras provokes premature cell senescence associated with accumulation of p53 and p16INK4a. *Cell* 88:593–602.
17. Tremain R, et al. (2000) Defects in TGF-beta signaling overcome senescence of mouse keratinocytes expressing v-Ha-ras. *Oncogene* 19:1698–1709.
18. Yeager TR, et al. (1998) Overcoming cellular senescence in human cancer pathogenesis. *Genes and Development* 12:163–174.
19. Denoyelle C, et al. (2006) Anti-oncogenic role of the endoplasmic reticulum differentially activated by mutations in the MAPK pathway. *Nat Cell Biol* 8:1053–1063.
20. Zhu B, et al. (2014) The nuclear receptor peroxisome proliferator-activated receptor-β/δ (PPARβ/δ) promotes oncogene-induced cellular senescence through repression of endoplasmic reticulum stress. *J Biol Chem* 289:20102–20119.
21. Yuspa SH, Dlugosz AA, Denning MF, Glick AB (1996) Multistage carcinogenesis in the skin. *J Investig Dermatol Symp Proc* 1:147–150.
22. Yang L, et al. (2010) A Phos-tag-based approach reveals the extent of physiological endoplasmic reticulum stress. *PLoS One* 5:e11621.
23. Ozcan U, et al. (2006) Chemical chaperones reduce ER stress and restore glucose homeostasis in a mouse model of type 2 diabetes. *Science* 313:1137–1140.
24. Cross BC, et al. (2012) The molecular basis for selective inhibition of unconventional mRNA splicing by an IRE1-binding small molecule. *Proc Natl Acad Sci USA* 109:E869–E878.
25. Urano F, et al. (2000) Coupling of stress in the ER to activation of JNK protein kinases by transmembrane protein kinase IRE1. *Science* 287:664–666.
26. Vijayachandra K, Higgins W, Lee J, Glick A (2009) Induction of p16ink4a and p19ARF by TGFbeta1 contributes to growth arrest and senescence response in mouse keratinocytes. *Mol Carcinog* 48:181–186.
27. Wang W, et al. (2002) Sequential activation of the MEK-extracellular signal-regulated kinase and MKK3/6-p38 mitogen-activated protein kinase pathways mediates oncogenic ras-induced premature senescence. *Mol Cell Biol* 22:3389–3403.
28. Deng Q, Liao R, Wu BL, Sun P (2004) High intensity ras signaling induces premature senescence by activating p38 pathway in primary human fibroblasts. *J Biol Chem* 279:1050–1059.
29. Lin AW, et al. (1998) Premature senescence involving p53 and p16 is activated in response to constitutive MEK/MAPK mitogenic signaling. *Genes Dev* 12:3008–3019.
30. So JS, et al. (2012) Silencing of lipid metabolism genes through IRE1α-mediated mRNA decay lowers plasma lipids in mice. *Cell Metab* 16:487–499.
31. Hur KY, et al. (2012) IRE1α activation protects mice against acetaminophen-induced hepatotoxicity. *J Exp Med* 209:307–318.
32. Cho JA, et al. (2013) The unfolded protein response element IRE1α senses bacterial proteins invading the ER to activate RIG-I and innate immune signaling. *Cell Host Microbe* 13:558–569.
33. Lipson KL, et al. (2006) Regulation of insulin biosynthesis in pancreatic beta cells by an endoplasmic reticulum-resident protein kinase IRE1. *Cell Metab* 4:245–254.
34. Ling F, Kang B, Sun XH (2014) Id proteins: Small molecules, mighty regulators. *Curr Top Dev Biol* 110:189–216.
35. Alani RM, Young AZ, Shifflett CB (2001) Id1 regulation of cellular senescence through transcriptional repression of p16/Ink4a. *Proc Natl Acad Sci USA* 98:7812–7816.
36. Swarbrick A, Roy E, Allen T, Bishop JM (2008) Id1 cooperates with oncogenic Ras to induce metastatic mammary carcinoma by subversion of the cellular senescence response. *Proc Natl Acad Sci USA* 105:5402–5407.
37. Wazir U, Jiang WG, Sharma AK, Newbold RF, Mokbel K (2013) The mRNA expression of inhibitors of DNA binding-1 and -2 is associated with advanced tumour stage and adverse clinical outcome in human breast cancer. *Anticancer Res* 33:2179–2183.
38. Diehn M, Bhattacharya R, Botstein D, Brown PO (2006) Genome-scale identification of membrane-associated human mRNAs. *PLoS Genet* 2:e11.
39. Jagannathan S, Nwosu C, Nicchitta CV (2011) Analyzing mRNA localization to the endoplasmic reticulum via cell fractionation. *Methods Mol Biol* 714:301–321.
40. Zuker M (2003) Mfold web server for nucleic acid folding and hybridization prediction. *Nucleic Acids Res* 31:3406–3415.
41. Lowry DT, Li L, Hennings H (1996) Thapsigargin, a weak skin tumor promoter, alters the growth and differentiation of mouse keratinocytes in culture. *Carcinogenesis* 17:699–706.
42. Prischi F, Nowak PR, Carrara M, Ali MM (2014) Phosphoregulation of Ire1 RNase splicing activity. *Nat Commun* 5:3554.
43. Lerner AG, et al. (2012) IRE1α induces thioredoxin-interacting protein to activate the NLRP3 inflammasome and promote programmed cell death under irremediable ER stress. *Cell Metab* 16:250–264.
44. Upton JP, et al. (2012) IRE1α cleaves select microRNAs during ER stress to derepress translation of proapoptotic Caspase-2. *Science* 338:818–822.
45. Polsky D, Young AZ, Busam KJ, Alani RM (2001) The transcriptional repressor of p16/Ink4a, Id1, is up-regulated in early melanomas. *Cancer Res* 61:6008–6011.
46. Ghosh R, et al. (2014) Allosteric inhibition of the IRE1α RNase preserves cell viability and function during endoplasmic reticulum stress. *Cell* 158:534–548.
47. Diamond I, Owolabi T, Marco M, Lam C, Glick A (2000) Conditional gene expression in the epidermis of transgenic mice using the tetracycline-regulated transactivators tTA and rTA linked to the keratin 5 promoter. *J Invest Dermatol* 115:788–794.
48. Chin L, et al. (1999) Essential role for oncogenic Ras in tumour maintenance. *Nature* 400:468–472.
49. Iwawaki T, Akai R, Yamanaka S, Kohno K (2009) Function of IRE1 alpha in the placenta is essential for placental development and embryonic viability. *Proc Natl Acad Sci USA* 106:16657–16662.
50. Kaser A, et al. (2008) XBP1 links ER stress to intestinal inflammation and confers genetic risk for human inflammatory bowel disease. *Cell* 134:743–756.
51. Mohammed J, et al. (2010) TGFbeta1-induced inflammation in premalignant epidermal squamous lesions requires IL-17. *J Invest Dermatol* 130:2295–2303.
52. Reiner A, Yekutieli D, Benjamini Y (2003) Identifying differentially expressed genes using false discovery rate controlling procedures. *Bioinformatics* 19:368–375.
53. Eisen MB, Spellman PT, Brown PO, Botstein D (1998) Cluster analysis and display of genome-wide expression patterns. *Proc Natl Acad Sci USA* 95:14863–14868.
54. Huang W, Sherman BT, Lempicki RA (2009) Systematic and integrative analysis of large gene lists using DAVID bioinformatics resources. *Nat Protoc* 4:44–57.